Available online at www.sciencedirect.com
ScienceDirect
Nuclear and Particle Physics Proceedings 00 (2024) 1–12
Nuclear and Particle Physics Proceedings

Exotics searches at ATLAS

Kristina Mihule, on behalf of the ATLAS Collaboration

CERN, Experimental Physics Department, CH-1211 Geneva 23, Switzerland

Abstract

Many theories beyond the Standard Model (SM) have been proposed to address several SM shortcomings, such as explaining why the Higgs boson is so light, the origin of neutrino masses, or the observed pattern of masses and mixing angles in the quark and lepton sectors. These beyond-the-SM extensions predict new particles or interactions directly accessible at the LHC. These proceedings will highlight recent searches based on the full Run 2 data collected by the ATLAS detector at the LHC with a centre-of-mass energy of 13 TeV.

Keywords: ATLAS experiment, Beyond the Standard Model Physics (BSM), Exotics physics, Dark Matter (DM), Dark Photon, Beyond Standard Model Higgs boson, LHC

1. Introduction

Exotics physics has been searched for decades in experiments to answer the outstanding questions about elementary particles and fundamental interactions. The properties of the Standard Model (SM) particles have been successfully studied, allowing physicists to predict the expected SM processes with high accuracy. New, yet undiscovered physics beyond the Standard Model (BSM) can be found at collider experiments if an excess of events over the SM background prediction is observed. The ATLAS experiment [1] at the Large Hadron Collider (LHC) [2] at CERN (European Organisation of Nuclear Research) takes data from proton-proton (*pp*) collisions at unprecedentedly high energies and large instantaneous luminosity.

In LHC Run 2 (2015-2018), the ATLAS experiment collected an integrated luminosity of 140 fb^{-1} [3], and this amount of data provides more sensitivity to discover BSM physics than the data previously collected by ATLAS. The ATLAS Collaboration has tested numerous BSM hypotheses.

These proceedings summarise the recent results of Exotics searches at ATLAS by analysis of the Run 2 ATLAS data which resulted in a significant increase of the exclusion limits for the parameters in several BSM models. It focusses on searches for dark mesons and massless dark photons. The search for BSM signatures in events with a hadronically decaying massive electroweak boson and large missing transverse energy is also presented. The presented analyses extended the Exotics physics probes to the higher-mass and lower-production cross-section frontier.

2. ATLAS experimental setup

The ATLAS experiment is one of the two multipurpose detectors located at the beam crossing points in the LHC. The proton beams collided at a centre-of-mass energy of 13 TeV every 25 ns during LHC Run 2. The interaction point is surrounded by layers of sensitive detector material, enabling the identification and reconstruction of particles. The innermost Inner Detector (ID) placed into a superconducting solenoid recon-

*Plenary talk presented at the 27th International Conference in QCD "QCD24 - 35 years later", 8-12/07/2024, Montpellier, France

Email address: kristina.mihule@cern.ch (Kristina Mihule, on behalf of the ATLAS Collaboration)

structs tracks left by passing electrically charged particles. The electromagnetic Liquid Argon calorimeter registers, primarily, electrons and photons. The hadronic calorimeters contribute to the detection of jets, hadronically decaying τ-leptons, and hadrons. The outermost Muon Spectrometer (MS) with three toroidal magnets measures tracks of muons whose identification is based on the combination of input from the ID and MS. Multiple ATLAS subdetectors pass the data to the two-level trigger system [4] which decides whether a given event will be stored for future analyses. The recorded collision events are reconstructed [5], providing information on the physical objects: electrons, photons, muons, jets, hadrons, hadronically decaying τ-leptons, – and a wide range of event observables.

3. Motivation for ATLAS BSM searches in events with large missing transverse energy

If being produced in proton-proton collisions at the LHC, BSM particles can interact via new forces and pass through the detector matter undetected. Although these particles do not leave a direct trace in the detector, their production can be identified as a momentum imbalance in the transverse plane, which is called missing transverse energy ($E_{\mathrm{T}}^{\mathrm{miss}}$). $E_{\mathrm{T}}^{\mathrm{miss}}$ value is defined by the magnitude of the missing transverse momentum $\vec{p}_{\mathrm{T}}^{\,\mathrm{miss}}$ as follows [6]:

$$\vec{p}_{\mathrm{T}}^{\,\mathrm{miss}} = -\sum_{\substack{\text{selected}\\ \text{electrons}}} \vec{p}_{\mathrm{T}} - \sum_{\substack{\text{accepted}\\ \gamma}} \vec{p}_{\mathrm{T}} - \sum_{\substack{\text{selected}\\ \mu}} \vec{p}_{\mathrm{T}} - \sum_{\substack{\text{accepted}\\ \tau_{\mathrm{h}}}} \vec{p}_{\mathrm{T}} - \sum_{\substack{\text{accepted}\\ \text{jets}}} \vec{p}_{\mathrm{T}} - \sum_{\substack{\text{soft}\\ \text{tracks}}} \vec{p}_{\mathrm{T}}. \quad (1)$$

In this way, the missing transverse momentum is reconstructed based on the set of the transverse momenta of the calibrated hard-scatter objects as well as the soft term defined with the transverse momenta of the tracks which are reconstructed but not associated with any from the above-mentioned calibrated objects.

One of the main goals of ATLAS is the observation of dark matter (DM) particles whose experimental detection would explain the cosmological evidence for the dark matter. Analyses of events with a large missing transverse energy are prospective in the search for dark-matter candidates in particular.

Since the discovery of a Higgs boson (H) [7, 8], an effort has been made to investigate the possible relation of the Higgs boson with BSM physics. Searching for (semi-)invisible Higgs boson decays is one method of probing Higgs boson coupling with the dark matter sector.

These proceedings emphasise the analyses of events with large missing transverse energy upon pp collisions that occurred during Run 2 ATLAS data-taking. The hypotheses of dark meson (π_D, ρ_D) and dark photon (γ_d) production were tested which allowed, among other results, to set stringent limits on the dark meson candidate mass and the branching ratio ($\mathcal{B}$) of Higgs boson decay $H \to \gamma\gamma_d$. The search for Exotics physics in events with a hadronically decaying massive electroweak boson and large missing transverse energy is presented, and this result is interpreted in terms of the limits on axion-like and weakly interacting particles models, along with the scenarios of dark-matter production in invisible Higgs boson decays as well as pseudo-scalar mediator decays within the two-Higgs doublet model.

4. Statistical Analysis

The discussed searches target the discovery of new particles based on the properties of recorded events and related physical objects.

The search for Exotics physics is performed in the phase space where the BSM signal under study is expected. This so-called signal region (SR) is usually defined with a series of event selections so that the fraction of SM contributions is reduced, which increases sensitivity to the BSM signal. Accurate prediction of SM background is crucial for BSM searches, and the contribution from leading SM background(s) is usually estimated in the orthogonal or statistically independent phase space(s) enriched with the given SM process; such a phase space is called a control region (CR). Another phase space populated with the SM process(es) can be used as a validation region to check the precision of the SM background prediction.

The searches can be performed in a single SR; however, multiple SRs can be considered to increase the sensitivity for the BSM signal. The model is simultaneously fitted to the observed data in all SRs and CRs using the profile likelihood method [9]. The likelihood includes terms for the probability of the expected event rate and statistical and systematic uncertainties. The likelihood is minimised to obtain the optimal values for the strength of the BSM signal, the uncertainties, and their estimated errors. The background-only fit implies testing whether there is a statistically significant discrepancy between the SM estimate and the collected data. Evidence (observation) of a new particle is claimed if the statistical significance of the excess above the SM expectation is above 3σ (5σ). If there is no statistically significant deviation from the SM prediction, the exclusion limits at 95% Confidence Level (CL) on the BSM production cross section or other BSM param-

eters are extracted using the CL_s method [10] during the fit to the SM background plus the BSM signal model.

5. Search for a massless dark photon in decays of SM Higgs boson $H \to \gamma\gamma_d$ and heavy BSM Higgs boson $H_{\text{BSM}} \to \gamma\gamma_d$

The branching ratio of the SM Higgs boson decays to undetectable particles in $H \to ZZ^* \to 4\nu$ is 0.4%, therefore the measurement of $H \to invis$ signature can hint at new physics mechanisms. The current limit on the invisible Higgs boson decay $H \to invis$ branching ratio is at the level of 10% [11, 12], suggesting that further searches of Higgs boson coupling to the dark sector are interesting. A possible scenario for exploring the coupling of the BSM dark sector coupling to H is the Higgs boson decays to an SM photon and a massless dark photon (γ_d) which is a gauge boson in the extra $U(1)_d$ group of the dark sector.[1] The ATLAS experiment searched for Higgs bosons that decay to an SM photon and a massless dark photon. In $H \to \gamma\gamma_d$, the ordinary photon leaves a well-definable experimental signature, while the presence of the dark counterpart can be understood as a large $E_{\text{T}}^{\text{miss}}$. This final state can also arise in decays of heavy BSM Higgs bosons $H_{\text{BSM}} \to \gamma\gamma_d$, allowing testing the H_{BSM} hypothesis.

ATLAS performed several searches for massless dark photons in decays of Higgs bosons generated in the following production modes:

- gluon-gluon fusion $gg\text{F} \to H \to \gamma + E_{\text{T}}^{\text{miss}}$ (Figure 1a) whose contribution is based from the RECAST-based [13] reinterpretation of the search for DM in association with a single energetic photon [14],
- vector-boson fusion $\text{VBF} \to Hqq \to \gamma + qq + E_{\text{T}}^{\text{miss}}$ (Figure 1b) whose contribution is estimated from Ref. [15] and extended with the $gg \to H$ and high-mass Higgs boson H_{BSM} production, and
- ZH production in $q\bar{q}$ scattering (Figure 1c) and gluon-gluon fusion (Figures 1d and 1e) yielding the final state $\gamma + E_{\text{T}}^{\text{miss}} + Z \to \gamma + E_{\text{T}}^{\text{miss}} + ll\,(l = e, \mu)$[2]; these contributions are extracted from Ref. [16].

All searches analyse events with an isolated photon and the missing transverse energy. The SR is defined

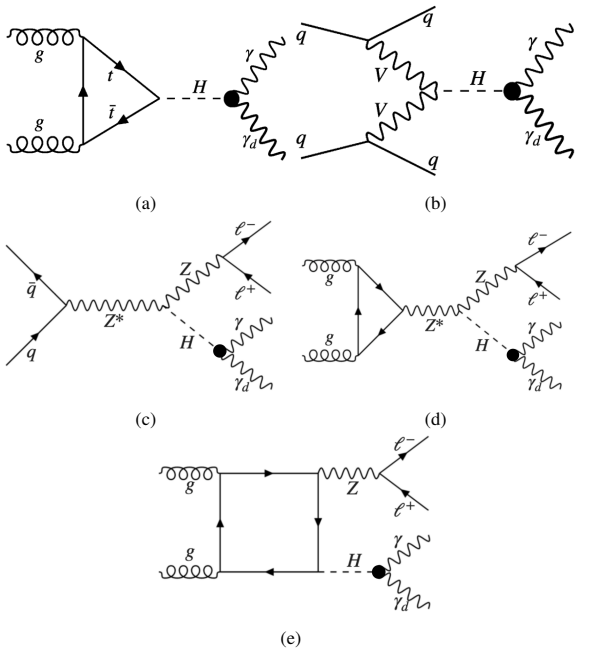

Figure 1: Feynman diagrams for the Higgs boson production in gluon-gluon fusion (a), vector-boson fusion (b), and in association with a Z boson in quark-antiquark scattering (c) and gluon-gluon fusion (d, e) with the Higgs boson subsequently decaying to a SM photon and a dark photon [17].

with selections on the trigger conditions $E_{\text{T}}^{\text{miss}}$, the transverse momentum of the photon E_{T}^{γ}, as well as the multiplicity of jets, leptons, etc. as listed in Table 1. The expected SM background is modelled with MC, and the dominating SM contributions are constrained in the dedicated CRs. The fake photon background resulting from jet and electron misidentification as well as the background arising from $E_{\text{T}}^{\text{miss}}$ are estimated with data-driven techniques.

No evidence for BSM physics was found in the individual searches. The presented combination [17] of the searches for $H \to \gamma\gamma_d$ is well motivated given the competitive results obtained by each of them.

The combinations consider two combination scenarios of the analyses mentioned above.

- The production of the SM Higgs boson $m_H = 125$ GeV is estimated in the combination of the VBF and ZH channels. As the Higgs boson production in association with jets in ggF brings a significant yield in certain SR phase spaces, the $gg \to H$ production mechanism is included in the VBF channel in this combination.
- The heavy Higgs boson ($m_{H_{\text{BSM}}} = 400 - 3000$ GeV) production is tested in the combined ggF and VBF

[1] The same experimental signature can be found in the case of the dark photon ultra-light dark photon.

[2] Hereinafter l denotes electrons and muons.

Table 1: The list of the main event selection, discriminating variables and the contributing processes in the considered VBF, ZH, and VBF channels [17]. Here, the centrality of an object i with respect to the leading j_1 and subleading j_2 jets is determined as $C_i = \exp[-\frac{4}{(\eta_{j_1}-\eta_{j_2})^2}(\eta_i - \frac{\eta_{j_1}+\eta_{j_2}}{2})^2]$.

Channels	VBF	ZH	ggF
Trigger	$E_{\mathrm{T}}^{\mathrm{miss}}$	Lepton(s)	Photon
Photons	$N_\gamma = 1, C_\gamma > 0.4$	$N_\gamma = 1$	$N_\gamma \geq 1$
E_{T}^{γ} [GeV]	$\in (15, \max(110, 0.733 \times m_{\mathrm{T}}))$	> 25	> 150
$E_{\mathrm{T}}^{\mathrm{miss}}$ [GeV]	> 150	> 60	> 200
Jets	$N_j = 2$ or $N_j = 3, m_{j_1 j_2} > 250$ GeV $\lvert\Delta\eta_{j_1 j_2}\rvert > 3, \eta_{j_1} \cdot \eta_{j_2} < 0$ $\Delta\phi_{j_1 j_2} < 2, C_{j_3} < 0.7$	$N_j \leq 2$	$N_j \leq 1$
Leptons	$N_l = 0$ (e, μ)	$N_l = 2$ of the same flavour and opposite electrical charge $m_{ll} \in (76, 116)$ GeV	$N_l = 0$ (e, μ, τ)

channels, in the theory with the additional high-mass Higgs boson in the narrow width approximation[3]. The VBF simulation was extended up to 3 TeV for this search combination to align with the mass range probed in the ggF analysis. For the search for the BSM Higgs boson, the $gg \rightarrow H_{\mathrm{BSM}}$+jets production was added to the VBF channel as it gathers a substantial contribution to the SR, specifically for the tested $m_{H_{\mathrm{BSM}}} < 1$ TeV [14].

The presence of the dark photon is characterised by the missing transverse energy, and $E_{\mathrm{T}}^{\mathrm{miss}}$ is used as a variable in the final combination fit. Figure 2 illustrates the $E_{\mathrm{T}}^{\mathrm{miss}}$ distribution in the SR under the $H_{\mathrm{BSM}} \rightarrow \gamma\gamma_d$ assumption. The channels analysed in the individual searches are taken as statistically independent as they impose different requirements on object multiplicity or employ different object reconstruction algorithms. In the search combination, the resulting likelihood function includes the systematic uncertainties of individual analyses, keeping uncertainties from common origins correlated. The common-origin uncertainties are, for example, the uncertainties associated with the data taking conditions (such as the uncertainty on the integrated luminosity measurement) and the uncertainties related to the physical objects analysed by several searches, e.g. the uncertainty on energy scale and energy resolution of jets reconstructed with the same algorithm [17].

[3]In the narrow width approximation, the total width of the heavy Higgs boson is assumed to be much smaller than its mass and the $pp \rightarrow H_{\mathrm{BSM}} \rightarrow \gamma\gamma_d$ cross section is factorised as the cross section of the H_{BSM} production and the decay width $\mathcal{B}(H_{\mathrm{BSM}} \rightarrow \gamma\gamma_d)$.

[3]The ATLAS coordinate system is a right-handed Cartesian one. The z-axis is directed along the beam line. The x-axis passes through the interaction point and the centre of the LHC ring, and the y-axis is pointed perpendicularly upwards. The cylindrical system of the (r, ϕ) coordinates is introduced in the transverse plane, where r is parallel to the x-axis and ϕ is the azimuthal angle raised from the z-axis. In terms of a polar coordinate θ in the longitudinal (x, y) plane, pseudorapidity is defined as $\eta = -\ln\tan(\theta/2)$.

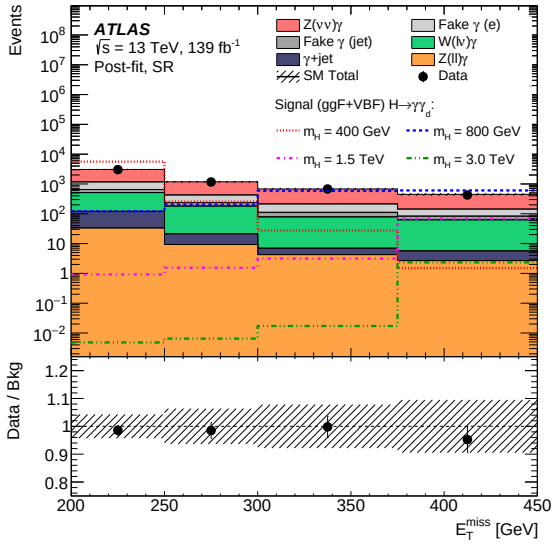

Figure 2: (The upper panel) The missing transverse energy $E_{\mathrm{T}}^{\mathrm{miss}}$ distribution in the SR, obtained in the background-only fit, in the analysis of $H_{\mathrm{BSM}} \rightarrow \gamma\gamma_d$ events. The ggF and VBF contribution to the Higgs boson production and $\mathcal{B}(H_{\mathrm{BSM}} \rightarrow \gamma\gamma_d) = 0.05$ are assumed. (The lower panel) The ratio between the observed data and the expected SM background [17].

In the $H \rightarrow \gamma\gamma_d$ search, the dominant systematic uncertainty comes from the background modelling (47%) and the calibration of jets and $E_{\mathrm{T}}^{\mathrm{miss}}$ (40%). The search for $H_{\mathrm{BSM}} \rightarrow \gamma\gamma_d$ encounters the statistical uncertainty between 75% and 86% in the higher BSM Higgs boson mass range and the fake-background uncertainty between 29% and 52% depending on the assumed H_{BSM} mass.

The observed 95% confidence level upper limit of the branching ratio $\mathcal{B}(H_{125} \rightarrow \gamma\gamma_d)$ is 1.3% (Figure 3) which is the most stringent constraint on $H \rightarrow \gamma\gamma_d$ at the LHC. The observed upper limit on $\sigma_{pp \rightarrow H_{\mathrm{BSM}}} \times \mathcal{B}(H_{\mathrm{BSM}} \rightarrow \gamma\gamma_d)$ is set to 1 fb (16 fb) for $m_H = 3$ TeV ($m_H = 400$ GeV) in the analysed $H \rightarrow \gamma\gamma_d$ event candidates. By assuming a theoretically predicted BSM Higgs boson production rate and $\mathcal{B}(H_{\mathrm{BSM}} \rightarrow \gamma\gamma_d) = 0.05$, the occurrence $H_{\mathrm{BSM}} \rightarrow \gamma\gamma_d$ was excluded for the mass H_{BSM} below ~ 1.6 TeV as shown in Figure 4.

Further, the result of the search combination is interpreted in the Minimal Model with two scalar messengers: one left $SU(2)$ doublet and one right $SU(2)$ singlet, which couple to both $U(1)$ and $U(1)_d$ fields. Therefore, $\gamma\gamma$, $\gamma\gamma_d$, and $\gamma_d\gamma_d$ Higgs boson decay modes through the scalar messenger are possible. The proportion between the individual branching ratios of these processes is determined by the mixing parameter between the right

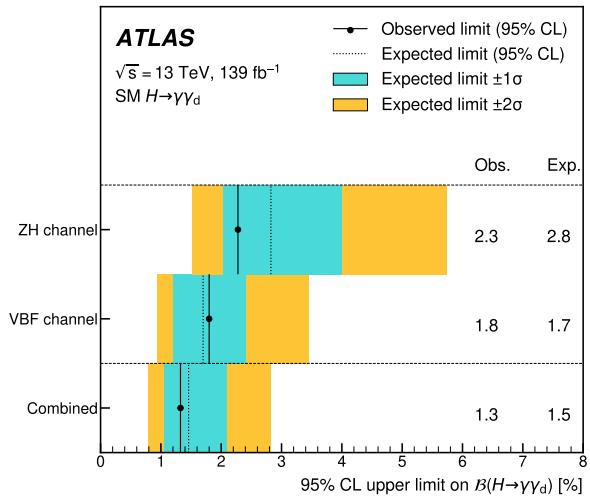

Figure 3: The observed and expected 95% CL upper limits on the Higgs boson decay branching ratio $\mathcal{B}(H \to \gamma\gamma_d)$ [17].

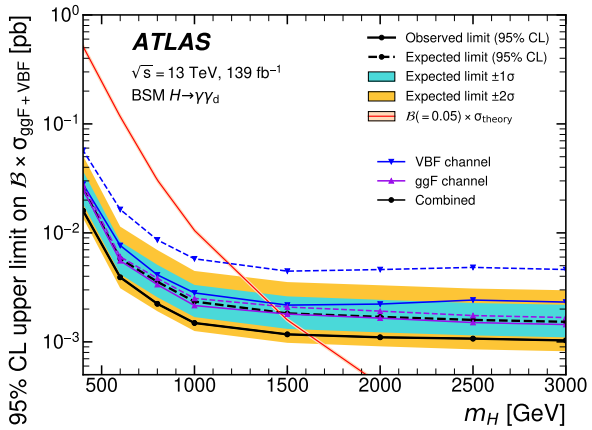

Figure 4: The upper limit on the cross section of the heavy Higgs boson decay $H_{\text{BSM}} \to \gamma\gamma_d$, assuming $\mathcal{B}(H_{\text{BSM}} \to \gamma\gamma_d) = 0.05$ and theoretically predicted H_{BSM} production cross section [17].

and left messengers ξ and α_d, which is the fine structure constant in the $U(1)_d$ group [18]. The region $\xi \geq 0.7$ at $\alpha_d = 1$ is excluded in the interpretation of invisible Higgs boson decays in terms of $H \to \gamma_d\gamma_d$, assuming constructive interference between the SM and the dark messenger sector[4].

6. Search for new physics phenomena in events with hadronic decays of the W or Z boson and large missing transverse energy

The search for BSM phenomena in events with large missing transverse energy and an associated hadronically decaying W or Z boson ($V \to q\bar{q}$[5]) provides a wide range of results on several BSM models [19].

The production of an axion-like particle (ALP) can lead to the final state with a massive electroweak SM boson and large $E_{\text{T}}^{\text{miss}}$ (Figure 5a) [20]. In addition, this signature can be interpreted as invisible Higgs boson decays (Figure 5d), production of a weakly interacting massive particle (WIMP) [21] mediated by a new axial or vector mediator [22] (Figure 5c), and as the $E_{\text{T}}^{\text{miss}} + Z$ production in the two-Higgs doublet model with a scalar mediator (2HDM+a) [23] (Figure 5b)[6]. Experimentally, in this type of events, the dark-sector or axion-like particles leave the signature of large $E_{\text{T}}^{\text{miss}}$ while recoiling against the SM particles which are well-traceable by the ATLAS detector.

The presented search for BSM particles in $E_{\text{T}}^{\text{miss}} + V(\to q\bar{q})$ events has several advantages over the previous one [24] which was based on the analysis of the partial Run 2 data set. The uncertainty in the presented search decreased with the larger amount of data collected and the increase in the size of the simulated samples for the SM background. The improved criteria for event selection and object reconstruction lead to the reduction of the related systematic uncertainties.

This search considers hadronic decay of the associated boson and analyses events that include no leptons. Depending on the Lorentz boost of the vector boson produced, two following decay topologies are distinguished:

- the merged regime with one large-radius jet ($R = 1.0$, $p_{\text{T}} > 250$ GeV) and $E_{\text{T}}^{\text{miss}} > 250$ GeV, and

[4]The model with destructive interference $\chi = -1$ was also studied, however, no limits can be set in this scenario with the analysed data.

[5]Hereinafter V denotes W and Z bosons.

[6]In the search for new physics in the 2HDM+a model only the production in association with the Z boson is considered as the production in association with the W boson yields small cross section.

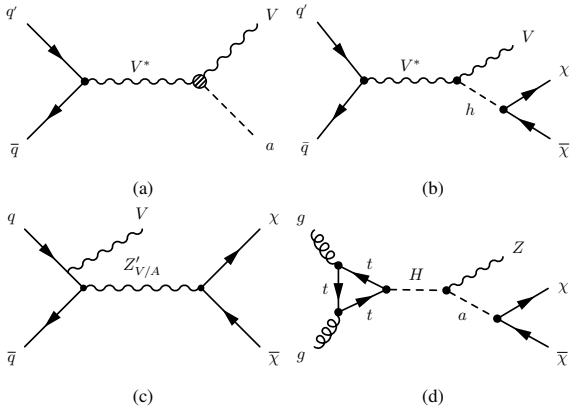

Figure 5: Feynman diagrams of the BSM interactions leading to the $E_{\mathrm{T}}^{\mathrm{miss}} + V$ final state: the axion-like particle production (a), invisible Higgs boson decay (b), scalar-mediator a decay in the 2HDM+a model (c), weakly-interacting particle production with a vector/axial mediator (d) [19].

- the resolved regime with two small-radius jets ($R = 0.4$) which have kinematic properties of the vector boson decay, namely $m_{j_1,j_2} \in [65, 105]$ GeV, $\Delta R_{j_1,j_2} < 1.4$, $\Delta\phi_{j_1,j_2} < 140^\circ$ where j_1 and j_2 denote the leading in p_{T} jet and subleading in p_{T} jet.

Boosted hadronically decaying vector bosons are reconstructed as large-radius ($R = 1.0$) jets. In this search, large-R jets are tagged as originating from hadronic vector boson decays (V tagged) based on the jet mass and the substructure variable D_2 [25] as well as the number of ID tracks that are ghost-associated with the jets [26] before jet grooming [27]. The merged SR is divided into the merged high-purity (MHP) and merged low-purity (MLP) regions, depending on whether the large-R jet candidate satisfies the V boson tagger parameters fully or partially.

The dominant source of the SM background is the production of $Z(\rightarrow \nu\nu)$ + jets, W + jets, and $t\bar{t}$. They are modelled with MC simulation. The $Z(\rightarrow \nu\nu)$+jets background is further constrained in the dileptonic phase space (ee and $\mu\mu$), while the contributions from W + jets and $t\bar{t}$ are corrected in single-muon events in the corresponding CRs distinguished by the number of b-jets. The normalisation factors for these SM contributions are derived in the CRs during the fit. The maximum likelihood fit is performed for the distribution of $E_{\mathrm{T},\not{}}^{\mathrm{miss}}$, which is the magnitude of the missing transverse momentum vector with leptons treated as invisible particles [19] defined as follows:

$$E_{\mathrm{T},\not{}}^{\mathrm{miss}} = |\boldsymbol{E}_{\mathbf{T},\not{}}^{\mathbf{miss}}| = |-\sum_{\substack{\text{object} \in \text{jet},\\ e,\mu,\tau}} \boldsymbol{p}_{\mathrm{T}}^{\text{object}} + \sum_{\substack{\text{soft}\\ \text{tracks}}} \boldsymbol{p}_{\mathrm{T}}^{\text{track}}|. \quad (2)$$

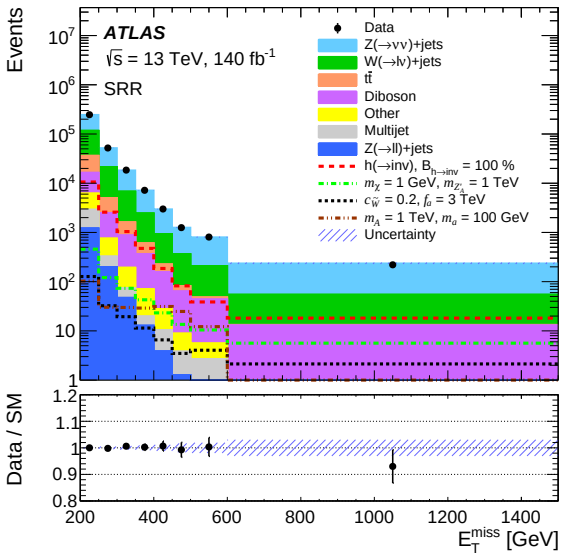

Figure 6: The missing transverse energy distribution $E_{\mathrm{T}}^{\mathrm{miss}}$ in the **s**ignal **r**egion with the **r**esolved (SRR) topology in $E_{\mathrm{T}}^{\mathrm{miss}} + V(\rightarrow q\bar{q})$ events, after the fit of the model to the data [19].

Table 2: Summary of the observed (expected) upper limits at 95% CL on the branching ratio of invisible Higgs boson decays $\mathcal{B}(H \rightarrow invis)$ [19].

Limits on $\mathcal{B}(H \rightarrow invis)$	Expected limit	Observed limit
Merged topology	$0.34^{+0.14}_{-0.09}$	0.38
Resolved topology	$0.54^{+0.23}_{-0.15}$	0.71
Combined	$0.31^{+0.13}_{-0.09}$	0.34

In events without leptons, such as those analysed in the SR, $\boldsymbol{E}_{\mathbf{T},\not{}}^{\mathbf{miss}}$ is identical to $\boldsymbol{E}_{\mathbf{T}}^{\mathbf{miss}}$. The variable $E_{\mathrm{T},\not{}}^{\mathrm{miss}}$ is used for the fit in the CRs. Among dominant uncertainties, there are those on large-R jets and the related V-tagging, V + jets modelling and the associated normalisation factors. The post-fit $E_{\mathrm{T}}^{\mathrm{miss}}$ distribution in the SR with the resolved topology is shown in Figure 6. The fit results in all SRs reveal the consistency of the SM background model with the observed data.

The presented analysis provides a range of experimental limits for multiple BSM models. The observed (expected) limit on the branching ratio of invisible Higgs boson decay is 0.34 (0.31) as summarised in Table 2. The merged topology shows better sensitivity to invisible Higgs boson decays. The result on the expected upper limit of $\mathcal{B}(H \rightarrow invis)$ is 1.9 factor better than the previous result obtained with 2015-2016 ATLAS data [24].

The model-independent upper exclusion limit at 95%

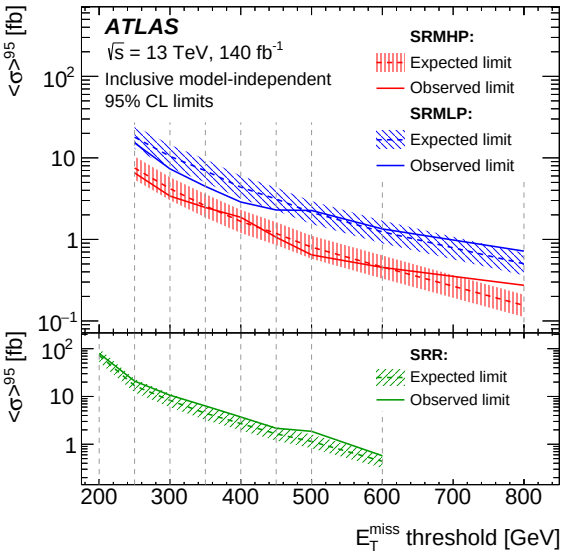

Figure 7: (The upper plot) The observed and expected model-independent upper limits on BSM processes visible cross section in $E_{\mathrm{T}}^{\mathrm{miss}} + V(\rightarrow q\bar{q})$ events, estimated in the SR with the merged jet topology of the high purity (SRMHP, depicted with blue) and low purity (SRMLP, depicted with red), where the purity is defined based on the V-tagger criteria [19]. The visible cross section is estimated as the production cross section convoluted with the signal acceptance and reconstruction efficiency. (The lower plot) The observed and expected model-independent upper limits on BSM processes cross section in $E_{\mathrm{T}}^{\mathrm{miss}} + V(\rightarrow q\bar{q})$ events, estimated in the SR with the resolved jet topology (SRR) [19].

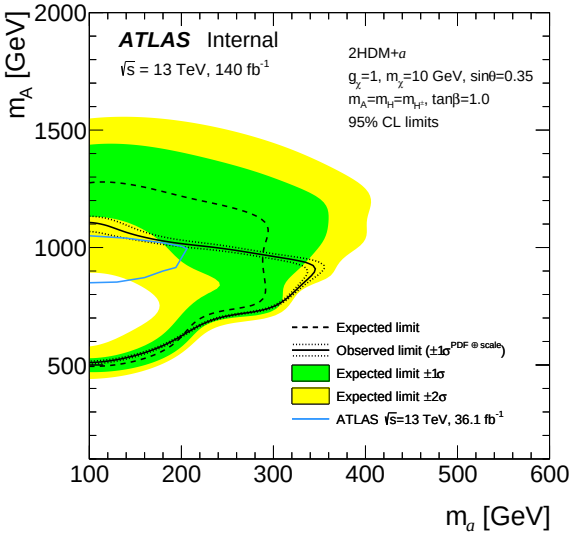

Figure 8: The observed and expected exclusion limits on the mass of pseudo-scalar mediator a and the pseudo-scalar Higgs sector state A within the 2HDM+a model, assuming the sinus of the mixing angle of the CP-odd weak eigenstates $\sin\theta = 0.35$, the masses of the pseudo-scalar (A), scalar (H), and charged Higgs bosons $m_A = m_H = m_{H^\pm}$, $g_\chi = 1$, the mass of the DM particle $m_\chi = 10$ GeV, and the ratio between the electroweak vacuum expectation values of the two Higgs doublets $\tan\beta = 1.0$ [19]. The previous result in the search with 36.1 fb^{-1} [24] is depicted with the blue solid line.

CL on the visible production cross section for the BSM phenomena in $E_{\mathrm{T}}^{\mathrm{miss}} + V(\rightarrow q\bar{q})$ events is shown in Figure 7. The visible cross-section limits vary from 79.5 fb to 0.3 fb when the MET threshold (indicated with the dashed grey vertical lines in Figure 7) increases from 220 GeV to 800 GeV. This result demonstrates a improvement compared to the predecessor analysis [24][7].

The search results were interpreted for the 2HDM+a model. Figure 8 illustrates the exclusion contour on the mass of the pseudo-scalar state in the Higgs doublet representation m_A and the mass of the pseudo-scalar dark-sector mediator m_a. For the assumed 2HDM+a parameters (see Figure 8), the values $m_a < 320$ GeV are excluded at 95% CL for $m_A = 900$ GeV, while the range $520 < m_A$ [GeV] < 1100 is excluded at 95% CL at $m_a = 100$ GeV.

The search tests, for the first time, the hypothesis on the generation of an axion-like particle in association with a V boson. The values of the ALP coupling with W boson $c_{\tilde{W}}$ above 0.1 are excluded, for the effective scale of ALP interactions $f_a = 1$ TeV (Figure 9). This result is obtained assuming an axion mass of 1 MeV, and the limits do not change significantly with the axion mass up to 1 GeV. The values $c_{\tilde{W}}/f_a > 0.11$ TeV^{-1} are excluded at 95% CL, which extends the current status of the limits on the coupling of ALP to W bosons.

Vector mediator masses up to 955 GeV are excluded for a dark-matter candidate mass of $m_\chi = 1$ GeV and a fixed choice of couplings (see Figure 10). The range below 965 GeV is excluded for the mass of an axial-vector mediator at $m_\chi = 1$ GeV. Both results extend the limits established in previous searches [24, 28]. The obtained limits were compared with the observations from the Planck [29] and WMAP [30] experiments. These cosmological estimates on the DM and mediator masses reach the exclusion region of the presented search at $m_{Z'_V} = 950$ GeV and $m_\chi = 97$ GeV for the vector mediator scenario and at $m_{Z'_V} = 750$ GeV and $m_\chi = 210$ GeV for the axial vector mediator scenario.

[7] Namely, the upper exclusion limit on the BSM production cross section was set to 69 – 185 fb for 150 GeV $< E_{\mathrm{T}}^{\mathrm{miss}} <$ 200 GeV and 9.2 – 9.7 fb for 400 GeV $< E_{\mathrm{T}}^{\mathrm{miss}} <$ 600 GeV in the search for $V(\rightarrow q\bar{q})$ + DM events [24] with the ATLAS 2015-2016 data set.

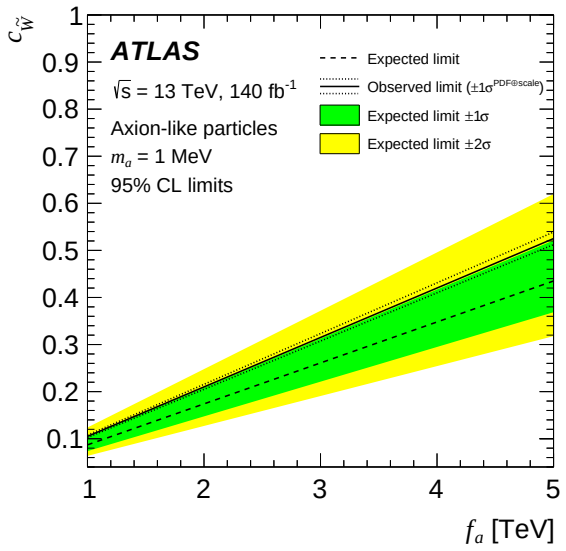

Figure 9: The observed and expected exclusion limits on the axion-like interaction effective scale f_a versus the coupling parameter $c_{\tilde{W}}$, for an ALP mass of 1 MeV [19].

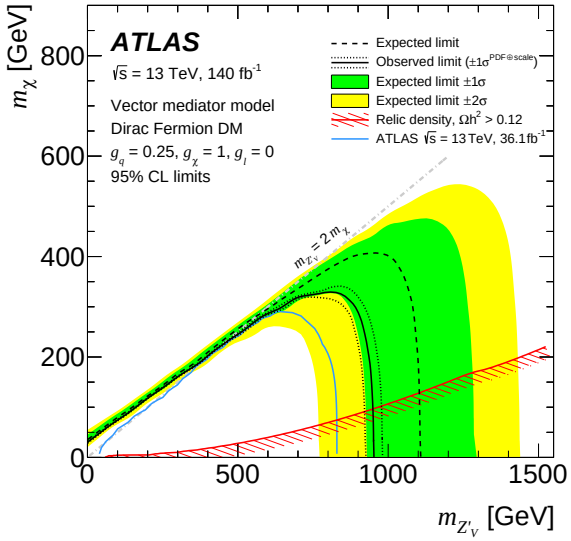

Figure 10: The observed and expected exclusion limits at 95% CL on the mass of the vector mediator (on the $x-$axis) and the dark matter candidate (on the $y-$axis) in the simplified dark matter model. The assumed values of the mediator couplings are the following: the coupling parameters to quarks $g_q = 0.25$, to DM particles $g_\chi = 1$, and to leptons $g_l = 0$ [19]. The parameters consistent with the Planck and WMAP measurements are depicted with the red line, the hashed side of which corresponds to the phase space if the relic density abundance is larger than the experimentally determined.

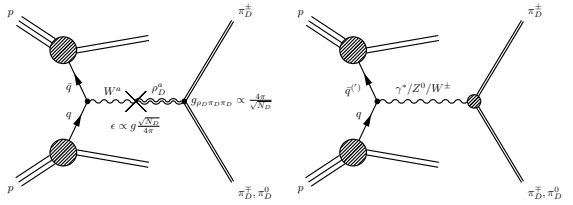

Figure 11: The production of the dark meson through the kinetic mixing with the W-boson (a) and in Drell-Yan process (b) [31].

7. Search for dark mesons decaying to top and bottom quarks

The SM can be extended with the strongly coupled dark sector with QCD-like flavour-conserving properties. This search [31] considers the Stealth Dark Matter model [32] where the new strongly coupled field is represented by vector-like fermions interacting with both the SM and dark sectors. In this model, dark mesons can be produced due to coupling to SM electroweak bosons, namely in the Drell-Yan process (Figure 11 (a)) or resonantly via kinetic mixing with electroweak gauge bosons (Figure 11 (b)). Due to the Higgs mechanism, dark mesons decay into SM states [33]. The targeted low-energy effective theory [34] predicts dark mesons whose production can take place at the LHC as well as stable dark-scalar baryons, which can be a candidate for the stable DM declared from cosmological measurements. This search targets the $SU(2)_L$[8] gauge-phobic model where dark meson decays to fermions (dark meson $\rightarrow f\bar{f}$ and dark meson $\rightarrow f\bar{f}'$) dominate over decays with associated W or Z bosons. The number of dark colours N_D is taken equal to 4 in this analysis, as is typically assumed in the Stealth Dark Matter [32] concept. A given dark pion mass and the ratio between the masses of the dark pion and the dark ρ-meson $\eta_D = m_{\pi_D}/m_{\rho_D}$ define the phenomenology of the model. The presented analysis, for the first time, targets models for $\eta_D < 0.5$, for which experimental limits are weaker than the exclusion limits for scenarios with $\eta_D > 0.5$, e.g. published in Refs. [35, 36].

Dark ρ-mesons decay to dark π-mesons which promptly decay to SM particles, as illustrated in Figure 12. For gaugephobic models, dark pions of mass above 200 – 400 GeV predominantly decay to the top and bottom quarks (Figure 13). In this way, the dark-

[8] The $SU(2)_R$ model of kinetic mixing of the dark meson with the SM would result in considerably smaller cross sections and is therefore not considered in the presented search.

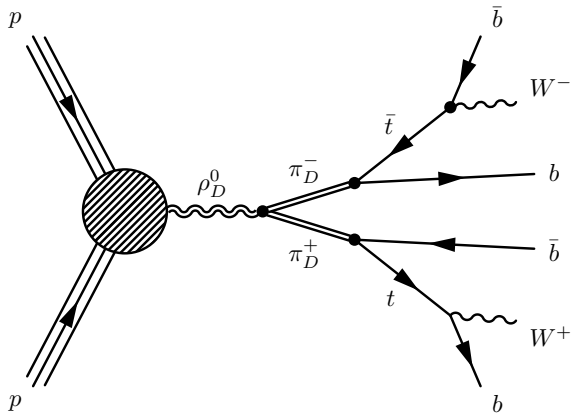

Figure 12: The illustration for the dark ρ-meson production in pp collisions followed by the decay to dark pions, which subsequently decay to SM top and bottom quarks [31].

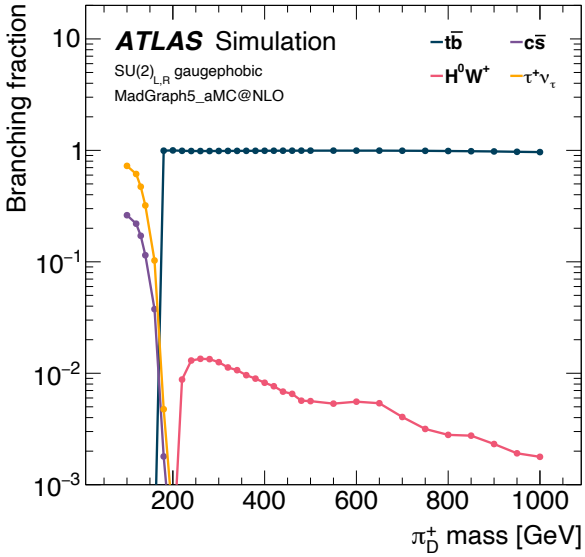

Figure 13: The assumed branching ratios for charged dark pion π_{D}^{+} decays in the $SU(2)_{L,R}$ gaugephobic model considered in the search [31].

meson production leads to the final states with multiple heavy-flavour quarks: $t\bar{t}b\bar{b}$ and $tttb$[9].

Experimentally, dark pions are identified as large-radius $R = 1.2$ jets (referred to as J). The large-R jets are reconstructed by reclustering standard-radius $R = 0.4$ jets (referred to as j) so that the former fully includes the decay products of dark mesons. This search concentrates on two decay channels of the top quarks:

- fully hadronic final states (referred as to the all-hadronic channel) collecting eight to ten jets, including at least four b-jets, and experimentally resulting in two fully hadronic large-R jets J^{had}, and
- final states with exactly one electron or muon (referred as to the 1-lepton channel) including multiple jets, from which four are from bottom quarks; this process leads to the signature with two large-R jets, namely one fully hadronic J^{had} and a one containing a light lepton J^{lep}.

In the all-hadronic channel, events are selected using the trigger on the transverse momenta of the reconstructed jets. Among other requirements, the selection of $m_{bb}/p_{\mathrm{T},bb} > 0.25$ suppresses the multijet background. Furthermore, the bb_i and $\pi_{D,i}$ tags define the SR, CR, and VR spaces.

- In the signal events, both jets should be contained within the large-R jet, therefore the bb_i tag sets the condition on the distance between the leading (subleading) jet and the second-closest b-jet: $\Delta R_{J_{1/2},b_2} < 1.0$.
- The leading and subleading large-R jet masses in the SR should satisfy the $\pi_{D,i}$ tag threshold, which is set to select the jets originating from the dark-pion decay: $m_{J_{1(2)}} > 300$ (250) GeV (Figure 14).

For the SR in the all-hadronic channel, the events should satisfy both tags for the two J^{had}. If three or two criteria out of the four bb_i and $\pi_{D,i}$ tags for J_1 and J_2 are met, the events form the CRs and VRs, respectively. The leading background in the all-hadronic channel is multi-jet production, estimated with the data-driven method. The extended ABCD method in this analysis (similar to the one used in [37]) employs 16 regions defined with four variables, corresponding to the conditions of the tags bb_i and π_{D_i} and their inversions. Other SM background contributions are estimated with Monte Carlo (MC) modelling. The SR is binned according to the leading and

[9] The states $tttb$ with three top quarks and one bottom quark include $t\bar{t}t\bar{b}$ and its charge conjugate $\bar{t}tb\bar{t}$.

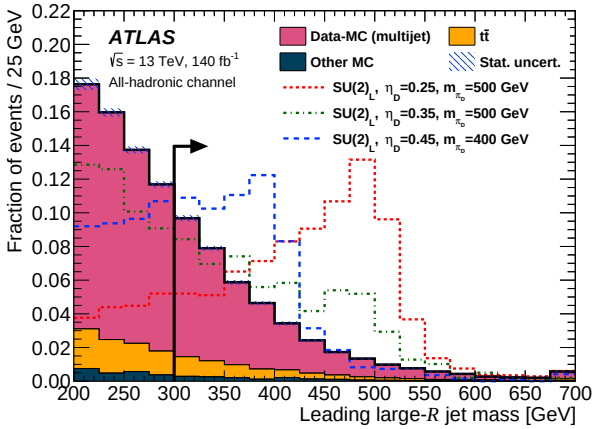

Figure 14: The distribution of the leading in p_{T} large-R jet mass for the SM background expectation (estimated here as the difference of the observed data and the background expectation, in a simplified manner) and three signal simulations for a chosen combination of the dark π-mesons mass m_{π_D} and the dark meson mass ratio $\eta + D$. While the low-m_{J_1} region is populated with SM processes, the dark-meson production is expected to dominate in the $m_{J_1} > 300$ GeV range, according to the assumed model [31].

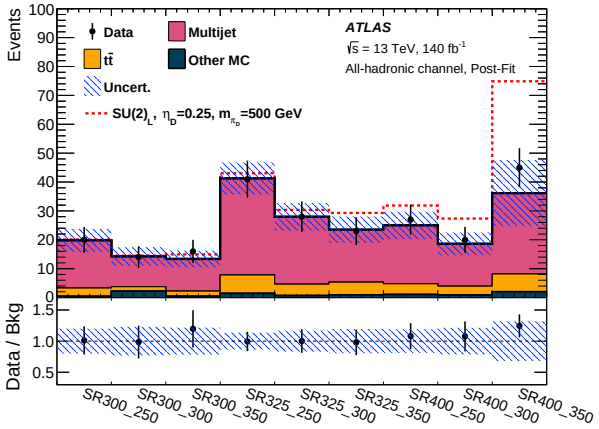

Figure 15: (The upper plot) The post-fit event rates in the SR bins of the all-hadronic channel. The event yields are depicted for the observed data, the expected SM background, and the simulated dark-meson signal ($m_{\pi_D} = 500$ GeV and $\eta_D = 0.25$). The SRs bins (on the x-axis) are indicated with two numbers standing for the lower boundary on the masses of the large-R masses: the first and the second numbers label the $m_{J_1^{\mathrm{had}}}$ and $m_{J_2^{\mathrm{had}}}$ lower boundaries, respectively [31]. (The lower plot) The ratio of the yields between the collected data and the expected SM background across the SRs analysed in the search for dark mesons in the $SU(2)_L$ QCD-like dark sector model, assuming $m_{\pi_D}/m_{\rho_D} = 0.25$ and $m_{\pi_D} = 500$ GeV.

subleading J masses to improve the discrimination of the BSM signal versus the SM background. The main uncertainty is the systematic uncertainty on the data-driven multi-jet background estimation. The fit results in the SRs of the all-hadronic channel are illustrated in Figure 15. The expected SM contribution agrees well with the observed event rates, disfavoring the hypothesis of the presence of dark-meson signals.

In the 1-lepton channel, the SR events are selected with the conditions on the corresponding single-lepton triggers. Several selections ensure that events have the topology of the leptonically decaying top quark stemming from the dark-pion decay.

- The angle between the lepton and the second closest to the lepton b-jet is expected to be small: $\Delta R(l, b_2) < 2.7$).
- The invariant mass of the two closest to each other b-jets should be above the energetic threshold so that the sum of the masses of the clustered jets corresponds to the mass of the decaying dark pion: $m_{\mathrm{bb,min\Delta R}} > 100$ GeV (Figure 16).

The dominating SM contribution in the 1-lepton channel – $t\bar{t}$ and $t\bar{t}$ + HF production – is modelled with MC simulation. The phase spaces orthogonal to the SR are employed as control and validation regions for the $t\bar{t}$ + jets background. Two normalisation factors – $t\bar{t}+ \geq 1b$ and $t\bar{t}$ + light and $t\bar{t}$ + c contribution – are estimated in the CRs during the fit. The analysed signal phase space is further split into several SRs according to the jet and b-jet multiplicity. Statistical analysis is performed with the fit to the sum of the masses of the two jets $m_{J^{\mathrm{had}}} + m_{J^{\mathrm{lep}}}$ as this sum proxies the mass of the decaying dark pion. The theoretical uncertainty in the background modelling dominates the total uncertainty. Figure 17 displays the post-fit $m_{J^{\mathrm{had}}} + m_{J^{\mathrm{lep}}}$ spectrum in one of the SRs in the 1-lepton channel, which shows no excess over the predicted SM background.

The collected data and the SM background prediction are in good agreement, and there was no evidence of dark meson presence according to the benchmark model in the ATLAS Run 2 data set. This search established the first direct constraints on the dark model with QCD-like flavour-conserving properties, assuming $m_{\pi_D}/m_{\rho_D} < 0.5$. Figure 18 shows the observed and expected exclusion contours at the 95% confidence level for the DM model under consideration. The one-lepton contour contains the all-hadronic one due to the higher sensitivity to the signal in the former. This search sets the best for the moment exclusion limits on the dark ρ-meson and dark pion masses: for $m_{\pi_D}/m_{\rho_D} < 0.45$ (0.25), the production of dark pions with $m_{\pi}^{\mathrm{DM}} < 943$ (738) GeV is excluded in the analysed data.

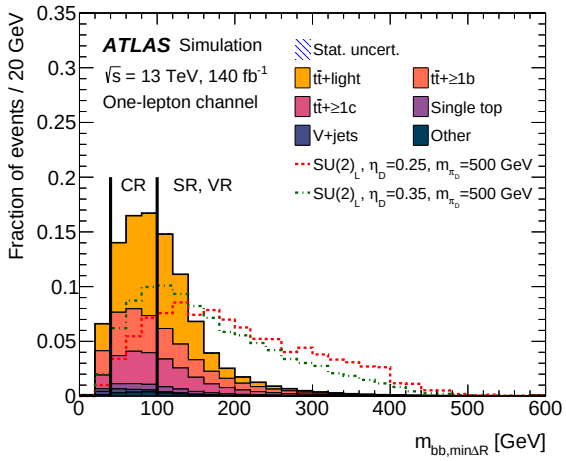

Figure 16: The distribution of $m_{\mathrm{bb,minΔR}}$ labelling the invariant mass of the two b-jets closest to each other in terms of ΔR. While the low-$m_{\mathrm{bb,minΔR}}$ $<$ 100 GeV region is populated with SM processes, the dark-meson production is expected to dominate in the $m_{\mathrm{bb,minΔR}}$ $>$ 100 GeV range, according to the assumed model. The validation region is defined in events with $m_{\mathrm{bb,minΔR}}$ $>$ 100 GeV and $2.7 < \Delta R(l, b_2) < 3.5$ (i.e. the selection inverted with respect to the SR) [31].

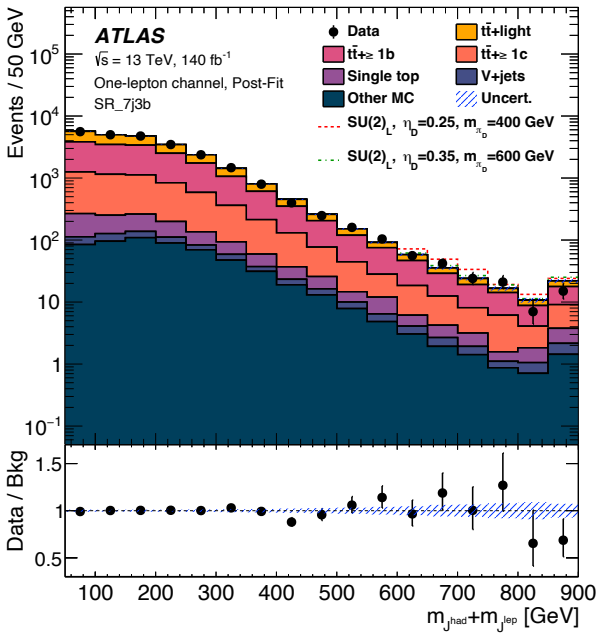

Figure 17: (The upper plot) The $m_{J\mathrm{had}} + m_{J\mathrm{lep}}$ distribution in the 1-lepton SR with seven jets from which three are b-quark tagged (SR_7j3b). The distribution in the observed data, the post-fit modelled SM background, and the simulated $SU(2)_L$ dark meson signal at $m - \pi_D = 400$ GeV and $\eta_D = 0.25$ are shown. (The lower plot) The ratio between the observed data and the expected SM background, after the background-only fit performed [31].

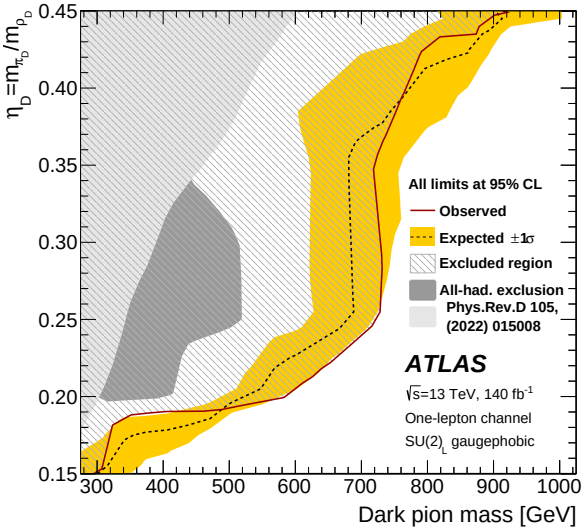

Figure 18: The observed and expected limits on the dark meson model in events with $t-$ and $b-$quarks in the 2D plane: the assumed dark meson versus the $\eta_{\mathrm{D}} = m_{\pi_{\mathrm{D}}}/m_{\rho_{\mathrm{D}}}$ [31].

8. Conclusion

The data collected during the ATLAS experiment provide material for the searches for BSM physics. The ATLAS Exotics programme tests multiple BSM models to find evidence of new particle production in the collected data or otherwise set limits on new physics models.

In the presented searches for Exotics particles, no significant excess is observed above the SM prediction. The exclusion limits obtained on $H \to \gamma\gamma_d$, 2HDM+a, ALPs, WIMPs, dark-matter mediators, among others, are more stringent than the previous results. For the first time, the search for dark mesons was performed, assuming $m_{\pi_D}/m_{\rho D} < 0.5$ and the hypothesis of the production of axion-like particles in association with a V boson was tested. The experiment established the most stringent to date constraints on the search for $H \to \gamma\gamma_d$. Data are being collected at the LHC in the ongoing Run 3. With continuously improving reconstruction and selection techniques, combined analyses for gaining statistical power, and many other efforts, the ATLAS Collaboration continues to pursue finding BSM physics.

References

[1] ATLAS Collaboration. The ATLAS Experiment at the CERN Large Hadron Collider. *J. Instrum.*, 3:S08003, 2008.
[2] L. Evans and P. Bryant (editors). LHC Machine. *J. Instrum.*, 3:S08001, 2008.

[3] ATLAS Collaboration. Luminosity determination in pp collisions at $\sqrt{s}$ = 13 TeV using the ATLAS detector at the LHC. *Eur. Phys. J. C*, 83(10), October 2023.

[4] ATLAS Collaboration. Performance of the ATLAS trigger system in 2015. *Eur. Phys. J. C*, 77:317, May 2017.

[5] ATLAS Collaboration. Software and computing for Run 3 of the ATLAS experiment at the LHC. `http://arxiv.org/abs/2404.06335`, April 2024. arXiv:2404.06335.

[6] ATLAS Collaboration. The performance of missing transverse momentum reconstruction and its significance with the ATLAS detector using 140 fb^{-1} of $\sqrt{s}$ = 13 TeV pp collisions. `https://arxiv.org/abs/2402.05858`, April 2024. arXiv:2402.05858.

[7] ATLAS Collaboration. Observation of a new particle in the search for the Standard Model Higgs boson with the ATLAS detector at the LHC. *Phys. Lett. B*, 716(1):1–29, September 2012.

[8] CMS Collaboration. Observation of a new boson at a mass of 125 GeV with the CMS experiment at the LHC. *Phys. Lett. B*, 716(1):30–61, September 2012.

[9] G. Cowan. Use of the profile likelihood function in searches for new physics. In *PHYSTAT 2011*, pages 109–114, Geneva, 2011. CERN. 10.5170/CERN-2011-006.109.

[10] A. L. Read. Presentation of search results: the CL_s technique. *J. Phys. G*, 28(10):2693, September 2002.

[11] CMS Collaboration. A portrait of the Higgs boson by the CMS experiment ten years after the discovery. *Nature*, 607(7917):60–68, July 2022.

[12] ATLAS Collaboration. A detailed map of Higgs boson interactions by the ATLAS experiment ten years after the discovery. *Nature*, 607(7917):52–59, July 2022.

[13] K. Cranmer and I. Yavin. RECAST — extending the impact of existing analyses. *J. High Energy Phys.*, 2011(4), April 2011.

[14] ATLAS Collaboration. Search for dark matter in association with an energetic photon in pp collisions at $\sqrt{s}$=13 TeV with the ATLAS detector. *J. High Energy Phys.*, 2021(2), February 2021.

[15] ATLAS Collaboration. Observation of electroweak production of two jets in association with an isolated photon and missing transverse momentum, and search for a Higgs boson decaying into invisible particles at 13 TeV with the ATLAS detector. *Eur. Phys. J. C*, 82(2), February 2022.

[16] ATLAS Collaboration. Search for dark photons from Higgs boson decays via ZH production with a photon plus missing transverse momentum signature from pp collisions at $\sqrt{s}$ = 13 TeV with the ATLAS detector. *J. High Energy Phys.*, 2023(7), July 2023.

[17] ATLAS Collaboration. Combination of searches for Higgs boson decays into a photon and a massless dark photon using pp collisions at $\sqrt{s}$ = 13 TeV with the ATLAS detector. *J. High Energy Phys.*, 2024(8), August 2024.

[18] S. Biswas *et al.* Dark photon searches via higgs boson production at the lhc and beyond. *Symmetry*, 14(8):1522, July 2022.

[19] ATLAS Collaboration. Search for new particles in events with a hadronically decaying W or Z boson and large missing transverse momentum at $\sqrt{s}$ = 13 TeV using the ATLAS detector. `http://arxiv.org/abs/2406.01272`, 2024. arXiv:2406.01272.

[20] I. Brivio *et al.* ALPs effective field theory and collider signatures. *Eur. Phys. J. C*, 77(8), August 2017.

[21] G. Bertone *et al.* Identifying WIMP dark matter from particle and astroparticle data. *J. Cosmol. Astropart. Phys.*, 2018(03):026–026, March 2018.

[22] D. Abercrombie *et al.* Dark Matter benchmark models for early LHC Run-2 Searches: Report of the ATLAS/CMS Dark Matter Forum. *Phys. Dark Universe*, 27:100371, January 2020.

[23] M. Bauer *et al.* Simplified dark matter models with two Higgs doublets: I. Pseudoscalar mediators. *J. High Energy Phys.*, 2017(5), May 2017.

[24] ATLAS Collaboration. Search for dark matter in events with a hadronically decaying vector boson and missing transverse momentum in pp collisions at $\sqrt{s}$ = 13 TeV with the ATLAS detector. *J. High Energy Phys.*, 10:180, October 2018.

[25] A. J. Larkoski *et al.* Power counting to better jet observables. *J. High Energy Phys.*, 2014(12), December 2014.

[26] M. Cacciari *et al.* The catchment area of jets. *J. High Energy Phys.*, 2008(04):005–005, April 2008.

[27] D. Krohn *et al.* Jet trimming. *J. High Energy Phys.*, 2010(2), February 2010.

[28] ATLAS Collaboration. Constraints on mediator-based dark matter and scalar dark energy models using $\sqrt{s}$ = 13 TeV pp collision data collected by the ATLAS detector. *J. High Energy Phys.*, 2019(5), May 2019.

[29] Planck Collaboration. Planck 2018 results: VI. Cosmological parameters. *Astron. Astrophys.*, 641:A6, September 2020.

[30] G. Hinshaw *et al.* Nine-years Wilkinson microwave anisotropy probe (WMAP observations): cosmological parameter results. *Astrophys. J. S*, 208(2):19, September 2013.

[31] ATLAS Collaboration. Search for dark mesons decaying to top and bottom quarks in proton-proton collisions at $\sqrt{s}$ = 13 TeV with the ATLAS detector. *J. High Energy Phys.*, 2024(9), 2024.

[32] T. Appelquist *et al.* Stealth dark matter: Dark scalar baryons through the Higgs portal. *Phys. Rev. D*, 92(7), October 2015.

[33] G. D. Kribs *et al.* Dark mesons at the LHC. *J. High Energy Phys.*, 2019(7), July 2019.

[34] G. D. Kribs *et al.* Effective theories of dark mesons with custodial symmetry. *J. High Energy Phys.*, 2019(8), August 2019.

[35] ATLAS Collaboration. Search for new high-mass phenomena in the dilepton final state using 36 fb^{-1} of proton-proton collision data at $\sqrt{s}$ = 13 TeV with the ATLAS detector. *J. High Energy Phys.*, 2017(10), October 2017.

[36] CMS Collaboration. Search for high-mass resonances in dilepton final states in proton-proton collisions at $\sqrt{s}$ = 13 TeV. *J. High Energy Phys.*, 2018(6), June 2018.

[37] ATLAS Collaboration. Measurements of $t\bar{t}$ differential cross-sections of highly boosted top quarks decaying to all-hadronic final states in pp collisions at $\sqrt{s}$ = 13 TeV using the ATLAS detector. *Phys. Rev. D*, 98(1):012003, July 2018.